PHYSICAL REVIEW B VOLUME 57, NUMBER 12 15 MARCH 1998-II

Optical anisotropy in arrow-shaped InAs quantum dots

M. Henini
Department of Physics, University of Nottingham, University Park, Nottingham NG7 2RD, United Kingdom

S. Sanguinetti,* S. C. Fortina, E. Grilli, and M. Guzzi
Istituto Nazionale per la Fisica della Materia and Dipartimento di Scienza dei Materiali, Università degli Studi di Milano, Via Emanueli 15, I-20126 Milano, Italy

G. Panzarini and L. C. Andreani
Istituto Nazionale per la Fisica della Materia and Dipartimento di Fisica ''A. Volta,'' Università di Pavia, I-27100 Pavia, Italy

M. D. Upward, P. Moriarty, P. H. Beton, and L. Eaves
Department of Physics, University of Nottingham, University Park, Nottingham NG7 2RD, United Kingdom

(Received 7 August 1997; revised manuscript received 19 December 1997)

We have observed a direct correlation between nonspherical shape and polarization anisotropy of optical transitions in quantum dots. The dots, grown by self-assembling during epitaxial deposition of InAs on GaAs(311)*A*, exhibit a nonconventional, faceted, arrowheadlike shape aligned in the [233] direction. The dot photoluminescence emission is partially ($\approx$13%) polarized along the same [233] direction. The presence and the sign of the emission polarization is in agreement with the predictions of a theoretical model. Full morphological and optical characterization is reported. [S0163-1829(98)52712-9]

The quest for high performance optoelectronic devices has led to a growing interest in zero-dimensional heterostructures [or quantum dots (QDs)] that exhibit atomiclike electronic characteristics. Due to wave-function localization effects, the electronic levels of QDs become quantized thus concentrating the oscillator strength on δ-like transitions.

The possibility of realizing such objects during epitaxial deposition of strained layers (Stranski-Krastanov growth) has been investigated in recent years.[1–5] This method requires a moderate lattice mismatch (2–8 %) between the QD material and the substrate and allows for the formation of dislocation-free QDs.

Key design parameters for QDs include size, shape, density, and spatial arrangement. After choosing the material system that allows QD formation, design flexibility is limited by the growth physics, usually determined by the temperature and growth rate of the epilayer. An alternative approach to influence the growth mode is to use high Miller index surfaces.[6–11] These provide different chemical potentials for the deposited species and thus affect the kinetics of adsorption, migration, and desorption. Besides, the particular substrate orientation and reconstruction determines the strain relaxation mechanism. These effects have a large impact on the range of achievable island shapes, sizes, and ordering.[12,13] The electronic levels are, in turn, determined by the QD shape and size: the correlation between design parameters, electronic structure, and optical properties is one of the main focuses of research in QD physics.

We have obtained self-assembled InAs QDs of highly nonconventional shape by using a GaAs(311)*A* substrate. Opposite to the QDs grown on (100) surfaces, where the shape ranges from round domes to square based pyramids, the (311)*A* dots display an arrowheadlike faceted shape. The arrow orientation is ordered and points along the [233] direction, which is related to a corrugation of (311)*A* surfaces.

We point out that there is a strict mutual relation between the nonspherical shape and the optical response in QDs. We will show that such an effect is due to the important role of valence-band degeneracy and valence-band mixing on the QD electronic wave function, which should not be omitted in electronic structure calculations. An adequate theoretical model was therefore developed, taking into account both surface orientation and shape anisotropy effects.

Shape anisotropy effects on the QD electronic properties are investigated here by measuring the polarization dependence of the optical transitions. We have found that the PL emission originating from QDs is preferentially polarized along the same [233] direction of the arrow tips. This result is in agreement with the prediction of our theoretical model. In addition to the fundamental interest for electronic structure and optical properties, the realization of a (partially) polarized light emitter might lend itself to applications in polarization-sensitive devices.

The sample under investigation was fabricated by molecular beam epitaxy deposition of InAs on liquid encapsulated Czochralski semi-insulating (311)*A* $\pm 0.5°$ GaAs substrate using a Varian Gen-II system. Simultaneously, identical structures were grown for comparison on a (100) $\pm 0.5°$ GaAs substrate. The grown structures consisted of the following layers, in order of growth from the substrate: a 0.3 mm thick undoped GaAs buffer followed by a 15 $\times$(3.8 nm $Al_{0.33}Ga_{0.67}As$+3.4 nm GaAs) superlattice, a 0.2 μm undoped GaAs, $\approx 1\times 10^{15}$ InAs molecules cm^{-2} (corresponding to 1.8 InAs monolayers on the reference sample), and a 30 nm undoped GaAs capping layer. The growth temperature was 630 °C as monitored by a pyrometer, except during the growth of InAs and capping layer when the temperature was lowered to 500 °C. The growth rates are one monolayer per second (ML/s) for GaAs, 0.5 ML/s for AlAs,

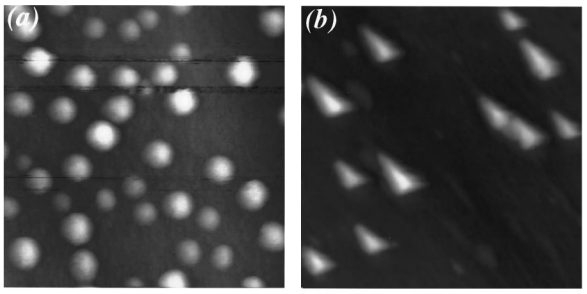

FIG. 1. STM pictures ($200\times200\ \mathrm{nm}^2$) of InAs/GaAs QD's grown on (100) (a) and (311)*A* (b) surfaces.

and 0.066 ML/s for InAs. After growth, the epitaxial surfaces were examined, using a Nomarski phase-contrast optical microscope and were found to be mirror smooth and nearly defect free. The size and density of InAs quantum dots were estimated by scanning tunneling microscope (STM) from samples of the same design but with the growth terminated after depositing the InAs layers. In addition a 0.5 μm Si-doped GaAs layer, doped to a level of $5\times10^{17}\ \mathrm{cm}^{-3}$, was grown before the growth of InAs quantum dots in order to provide the necessary carrier conduction for the STM experiment. For these samples, following growth of the InAs/GaAs structures, a protective amorphous As layer was deposited. The sample was then transferred, through air, to the UHV (STM) system. After degassing at 200 °C overnight, the protective As capping layer was thermally desorbed at 300 °C. It should be noted that, for all samples, there was no change in surface morphology following subsequent anneals up to a temperature of 350 °C.

Photoluminescence (PL) spectra were obtained in the 2–70 K range. The PL was excited with an Ar^+ laser, with power density in the range $1-1100\ \mathrm{W\ cm}^{-2}$. The spot diameter was in the range 100 to 400 μm. Luminescence spectra were measured with both a Fourier transform spectrometer operating with an $In_xGa_{1-x}As$ photodetector and a single grating monochromator with a cooled Ge detector. The polarization measurements were performed on the PL emitted normal to the surface via a Polaroid near infrared polarizer at the entrance slit of the grating monochromator and were corrected taking into account the system's optical response to polarized light.

Figure 1 shows representative STM images of GaAs(100) and (311)*A* samples: there are clear differences in the size, shape, and distribution of the InAs islands on the two substrates. While QDs grown on the (100) show the usual (for low coverage) isotropic, domelike shape, it is quite clear that the (311)*A* islands have a considerably more anisotropic and well developed faceted shape. The (311)*A* dot shape is arrowheadlike, and the dots are preferentially aligned along the [233] direction. This shape was checked not to be a STM tip artifact by scanning in orthogonal directions and by comparison against atomic force microscopy.

The (311) surface of GaAs has been shown to be corrugated with the formation of ''channels'' along the [233] axis and a lateral periodicity of 3.2 nm along the [011] direction.[14,15] The corrugation arises during epitaxial growth and is stable down to 300 K: it is associated to the breakup of the (311) surface into (331) and (313) facets, which form an angle of about 81°. Although the exact value of the step

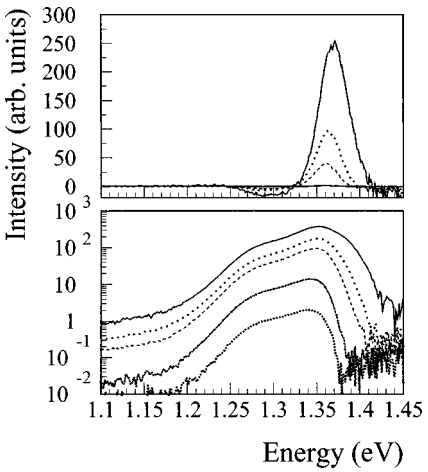

FIG. 2. Upper panel: difference between the spectrum taken at $1\ \mathrm{W\ cm}^{-2}$ excitation power density and spectra taken at higher excitation powers, normalized at 1.25 eV. Lower panel: photoluminescence spectra measured at 2 K using different excitation power densities. In both panels 1100 W cm^{-2} (continuous line), 280 W cm^{-2} (dotted), 100 W cm^{-2} (dashed), 10 W cm^{-2} (dash dotted), and 1 W cm^{-2} (short dotted).

height is debated,[14,15] the corrugated morphology is undoubtedly due to the lower energy of the (331) [compared to the (311)] surface, as indicated also by tight-binding calculations.[16] Lattice matched, weakly strained materials, or relaxed epilayers (e.g., AlAs, $In_xGa_{1-x}As$ or thick InAs epilayers) grown on the corrugated surface exhibit a lateral patterning with spatial periodicity along [011],[17,18] while the presence of strain due to a pseudomorphic InAs layer has been shown to suppress the corrugation.[19] Thus the scenario of QD formation is as follows: the pseudomorphic InAs wetting layer restores a flat surface, but, since in the present InAs dots the strain is partly relaxed,[20] the energetics of the InAs surface is such that breakup into (331) and (313) facets become favorable once again. This results in faceted InAs dots elongated along the [233] direction. Thus the combination of surface energetics [which makes the (311)*A* surface unstable] and partial residual strain in the InAs dots leads to the formation of self-organized dots with highly nonconventional shape.

The size distribution of the two samples, as determined from multiple STM images, is markedly different. The GaAs(100) sample shows a narrow distribution both in lateral and vertical size, while the GaAs(311)*A* sample has a much broader and multimodal distribution of sizes.[12]

For low excitation power density the PL line shape is determined by inhomogeneous broadening: PL spectra of these QD samples taken at 2 K with $1\ \mathrm{W\ cm}^{-2}$ excitation power density (Fig. 2) roughly reflect the corresponding size histograms. The (311)*A* multimodal distribution of sizes gives rise to the structured PL spectrum of this sample, while the GaAs(100) sample displays a single Gaussian peak (not shown) at 1.22 eV with a full width at half maximum (FWHM) of 60 meV. The integrated intensities of the two samples are comparable. In order to exclude band filling phenomena, which may affect PL spectral shape, the linearity of the PL intensity with the excitation power density has been tested, at 2 K, from 1 to $1100\ \mathrm{W\ cm}^{-2}$. Deviation from linearity starts at $100\ \mathrm{W\ cm}^{-2}$, where an additional PL line at

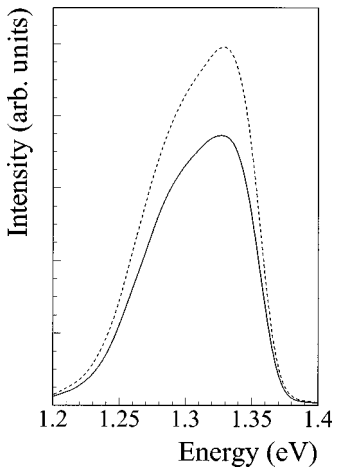

FIG. 3. Photoluminescence spectra measured at 10 K, collecting light polarized along the [233] (dotted line) and [011] (continuous) lattice directions.

1.37 eV (FWHM of 40 meV) begins to appear (Fig. 2). Following Grundmann *et al.*[21] we attribute this peak to the emission from an excited-state transition. The energy separation between this new transition and the one associated with recombination from dot ground states is of the same order (70 meV) as the reported value for GaAs(100) QDs.[21] The integrated intensity, for both (100) and (311)*A* samples, does not depend on temperature in the 2–70 K range.

PL polarization measurements were performed in the linear response regime with an exciting spot diameter of 400 μm. No PL polarization anisotropy was observed on the (100) reference sample. On (311)*A* the maximum intensity was reached at the detector when the Polaroid analyzer was parallel to the [233] direction (Fig. 3), the same direction of the arrow QD tips. The fraction of light polarized along [233] was $\rho=(I_{[\bar{2}33]}-I_{[01\bar{1}]})/(I_{[\bar{2}33]}+I_{[01\bar{1}]})=0.13\pm0.02$, where $I_{[\bar{2}33]}$ and $I_{[01\bar{1}]}$ are the integrated PL intensities along the two orthogonal directions [233] and [011], respectively. No noticeable temperature dependence of the polarization ratio has been observed in the 2–70 K range.

The size dependence of the emission polarization, being the PL linewidth dominated by inhomogeneous broadening, can be evaluated by looking at the energy dependence of the polarization ratio. No clear evidence of any size dependence has been observed. In fact, although the high-energy PL component of the spectrum has a mean polarization ratio ρ of $(2\pm3)\%$ higher than the low-energy component, the large standard deviation of the results gives to the null hypothesis (in this case no dependence on size of the PL polarization) a significance level as high as 15%. Thus a size dependence, if any, is very weak.

An explanation of the observed polarization anisotropy requires the consideration of the nonspherical QD shape as well as of the degeneracy of the valence bands in bulk III–V semiconductors. The valence-band top derived from atomic, *p* orbitals, when subject to quantum confinement in a nonspherical symmetry, gives rise to hole levels with strongly anisotropic charge distribution, which in turn produces polarization-dependent transitions to the *s*-like conduction band. Such effects have been thoroughly studied for quantum wells and quantum wires grown along conventional symmetry directions[22] or along (311) (Ref. 23) and more recently invoked for explaining polarization memory effects in porous silicon nanocrystals.[24] In the latter, however, the intrinsic random orientation of the nanocrystals prevents a direct observation of the correlation between spatial anisotropy and optical polarization properties.

A theoretical model should be based on a multiband envelope-function formalism in which the hole dynamics is treated by the Luttinger Hamiltonian[27] and the elongated shape of the (311)*A* QDs is taken into account. We have studied the polarization anisotropy in a model of rectangular quantum dots with infinite barriers for both conduction and valence bands; the hole levels are calculated for an arbitrary orientation of the QD sides with respect to the crystallographic axes, by expressing the Luttinger kinetic matrix in a rotated coordinate system and expanding the four-component spinors in a complete basis of confined wave functions along the three QD axes. This model (which will be presented in detail in a separate publication[25]) is adequate for describing the *change* of optical matrix element with polarization vector; we take realistic dot sizes (typically 20 nm along the [233] axis and 5 nm in the perpendicular plane) and sum over the transitions within our linewidth of few tens of meV. For cubic QDs we obtain an isotropic oscillator strength; on the other hand for a QD with dimension along [233] much larger than along the two perpendicular directions, we obtain a ground state which is light-hole-like, i.e., preferentially polarized along [233] with an anisotropy ratio $\rho=0.6$:[26] this has the same sign as in our experiment. In this limiting case of a quantum wire with the main axis along [233] our results are similar to those of Li and Xia.[28–30] The real situation is clearly intermediate between the two limiting cases of a cubic quantum box and a very elongated QD along [233]; therefore the observed polarization ratio ($\rho=0.13$) agrees with the theoretical expectations. Moreover, we find that the polarization ratio does not depend on a uniform scaling of QD size, again in agreement with the observations.

In conclusion, we have demonstrated that growth on a (311)*A* surface produces self-assembled QDs with different shape and optical properties. Due to a strain relaxation mechanism presumably governed by the energy balance between surface free energy and strain, the dots acquire an arrowheadlike shape pointing in the [233] direction. These QDs act as polarized emitters, with a noticeable fraction ($\approx$13%) of the total intensity polarized along the [233] direction. These results are in agreement with the theoretical model here developed for taking into account both surface orientation and shape anisotropy effects. No clear dependence of the polarization effect on the size has been observed, as expected by theory.

As a concluding remark, one of the leading effects of the anisotropic QD shape is to break the inversion symmetry in the surface plane of the localized electronic wave function. Such an effect, together with the predicted enhanced nonlinear optical properties,[31,32] make these dots promising candidates for second-harmonic generation.

We acknowledge helpful discussions with A. Bignazzi. The authors wish to thank E. Mastio and L. Brusaferri for help during the measurements. This work has been supported by the Engineering and Physical Sciences Research Council (EPSRC) in the United Kingdom. We acknowledge NATO for funds enabling the collaboration.

*Author to whom correspondence should be addressed. Electronic address: Stefano.Sanguinetti@mater.unimi.it

[1] J. M. Moison, F. Houzay, F. Barthe, L. Leprince, E. André, and O. Vatel, Appl. Phys. Lett. **64**, 196 (1994).

[2] J. Y. Marzin, J. M. Gérard, A. Izraël, D. Barrier, and G. Bastard, Phys. Rev. Lett. **73**, 716 (1994).

[3] D. Leonard, K. Pond, and P. M. Petroff, Phys. Rev. B **50**, 11 687 (1994).

[4] S. Ruvimov, P. Werner, K. Scheerschmidt, U. Gösele, J. Heydenreich, U. Richter, N. N. Ledentsov, M. Grundmann, D. Bimberg, V. M. Ustinov, A. Yu. Egorov, P. S. Kop'ev, and Zh. I. Alferov, Phys. Rev. B **51**, 14 766 (1995).

[5] J. Y. Marzin, J. M. Gerard, O. Cabrol, B. Jusserand, and B. Sermage, Nuovo Cimento D **17**, 1285 (1995).

[6] R. Nötzel, J. Temmyo, and T. Tamamura, Jpn. J. Appl. Phys., Part 2 **33**, L275 (1994).

[7] R. Nötzel, J. Temmyo, and T. Tamamura, Nature (London) **369**, 131 (1994).

[8] R. Nötzel, J. Temmyo, H. Kamada, T. Furuta, and T. Tamamura, Appl. Phys. Lett. **65**, 457 (1994).

[9] K. Nishi, R. Mirin, D. Leonard, G. Medeiros-Ribeiro, P. M. Petroff, and A. C. Gossard, J. Appl. Phys. **80**, 3466 (1996).

[10] D. I. Lubyshev, P. P. Gonzalez, E. Marega Jr., E. Petitprez, and P. Basmaji, J. Vac. Sci. Tech. B **14**, 2212 (1996).

[11] C. M. Reaves, R. I. Pelzel, G. C. Hsueh, W. H. Weinberg, and S. P. DenBaars, Appl. Phys. Lett. **69**, 3878 (1996).

[12] M. Henini, S. Sanguinetti, L. Brusaferri, E. Grilli, M. Guzzi, M. D. Upward, P. Moriarty, and P. H. Beton, Microelectron. J. **28**, 933 (1997).

[13] K. Nishi, T. Anan, A. Gomyo, S. Kohmoto, and S. Sugou, Appl. Phys. Lett. **70**, 3579 (1997).

[14] M. Wassermeier, J. Sudijono, M. D. Johnson, K. T. Leung, B. G. Orr, L. Däweritz, and K. Ploog, Phys. Rev. B **51**, 14 721 (1995).

[15] R. Nötzel, N. N. Ledentsov, L. Däveritz, M. Hohenstein, and K. Ploog, Phys. Rev. Lett. **67**, 3812 (1991).

[16] D. J. Chadi, Phys. Rev. B **29**, 785 (1984).

[17] E. Tourniè, R. Nötzel, and K. H. Ploog, Appl. Phys. Lett. **63**, 3300 (1993).

[18] E. Tourniè, R. Nötzel, and K. H. Ploog, Phys. Rev. B **49**, 11 053 (1994).

[19] M. Ilg, R. Nötzel, K. H. Ploog, and M. Hohenstein, Appl. Phys. Lett. **62**, 1472 (1993).

[20] M. Grundmann, O. Stier, and D. Bimberg, Phys. Rev. B **52**, 11 969 (1995).

[21] M. Grundmann, N. N. Ledentsov, O. Stier, J. Bohrer, D. Bimberg, V. M. Ustinov, P. S. Kop'ev, and Zh. I. Alferov, Phys. Rev. B **53**, R10 509 (1996).

[22] M. E. Portnoi, Sov. Phys. Semicond. **25**, 1294 (1992); C. R. McIntyre and L. J. Sham, Phys. Rev. B **45**, 9443 (1992); U. Bockelmann and G. Bastard, *ibid.* **45**, 1688 (1992); J. A. Kash *et al.*, Phys. Rev. Lett. **69**, 2260 (1992); F. Vouilloz, D. Y. Oberli, M.-A. Dupertuis, A. Gustafsson, F. Reinhardt, and E. Kapon, *ibid.* **78**, 1580 (1997).

[23] R. Nötzel M. Notomi, H. Kamada, T. Furuta, T. Yanagawa, and K. H. Plooget, Jpn. J. Appl. Phys., Part 1 **33**, 900 (1994).

[24] D. Kovalev, M. Ben-Chorin, J. Diener, B. Averboukh, G. Polisski, and F. Koch, Phys. Rev. Lett. **79**, 119 (1997).

[25] G. Panzarini, L. C. Andreani, and S. Sanguinetti (unpublished).

[26] The oscillator strength of a light-hole state is four times larger along the quantization axis than in the perpendicular plane, leading to $\rho = 3/5 = 0.6$.

[27] J. M. Luttinger, Phys. Rev. **102**, 1030 (1956).

[28] J. B. Xia, Phys. Rev. B **43**, 9856 (1991).

[29] S. S. Li and J. B. Xia, Phys. Rev. B **50**, 8602 (1994).

[30] J. B. Xia and S. S. Li, Phys. Rev. B **51**, 17 203 (1995).

[31] G. W. Bryant, Phys. Rev. B **37**, 8763 (1988).

[32] M. Sugarawa, N. Okazaki, T. Fujii, and S. Yamazaki, Phys. Rev. B **48**, 8848 (1993).